Quantifying the impact of scheduling and mobility on IR-UWB localization in body area networks

Arturo Guizar, Anis Ouni, C Goursaud, C Chaudet, Jean-Marie Gorce

Quantifying the Impact of Scheduling and Mobility on IR-UWB Localization in Body Area Networks

A. Guizar[†] [♯], A. Ouni[‡], C. Goursaud[†] [♯], C. Chaudet[‡], J.M. Gorce[†] [♯]
[♯]University of Lyon, INRIA
[†]INSA Lyon, CITI-INRIA, F-69621, Lyon, France
[‡]Institut Mines-Telecom - Telecom ParisTech - CNRS LTCI UMR 5141, F-75013, Paris, France
E-mails:{arturo.guizar, claire.goursaud, jean-marie.gorce}@insa-lyon.fr
{anis.ouni, claude.chaudet}@telecom-paristech.fr

***Abstract*—In the context of radiolocation in Wireless Body Area Networks (WBANs), nodes positions can be estimated through time-based ranging algorithms. For instance, the distance separating a couple of nodes can be estimated accurately by measuring the Round Trip Time of Flight of an Impulse Radio Ultra Wideband (IR-UWB) link. This measure usually relies on two or three messages transactions. Such exchanges take time and a rapid mobility of the nodes can reduce the ranging accuracy and consequently impact nodes localization process. In this paper, we quantify this localization error by confronting two broadcast-based optimized implementations of the three-way ranging algorithm with real mobility traces, acquired through a motion capture system. We then evaluate, in the same scenarios, the impact of the MAC-level scheduling of the packets within a TDMA frame localization accuracy. The results, obtained with the WSNet simulator, show that MAC scheduling can be utilized to mitigate the effect of nodes mobility.**

***Index Terms*—Body Area Networks, Mobility, positioning, Ranging, Ultra Wideband, Scheduling, Motion Capture**

I. Introduction

Wireless Body Area Networks (WBANs) are emerging as a key technology in many application domains, such as medicine, sports, civil security, and entertainment [1], [2]. These networks are capable of collecting and transmitting information on the activity of a person, based on the analysis of the body movement.

In the context of radiolocation applications, the Impulse Radio Ultra Wideband (IR-UWB) achieves a very good performance due to its high temporal and fine multipath resolution capabilities. It provides a high precision estimation of the Time-Of-Arrival (TOA) of transmitted signal [3]. The TOA is used by several ranging protocol like the 3-Way Ranging (3-WR) which consists in estimating the distance between a node and one of its neighbors using an exchange of three different packets: one request followed by two responses. However, depending on the wearer's movement speed, the positions of the mobile nodes may have changed before this exchange is complete, as illustrated by Figure 1. Positioning a node in a three dimensions space requires at least to measure distances with four of it neighbors. Estimation errors on all these links can easily accumulate, yielding to a coarse estimate of the node's position [4].

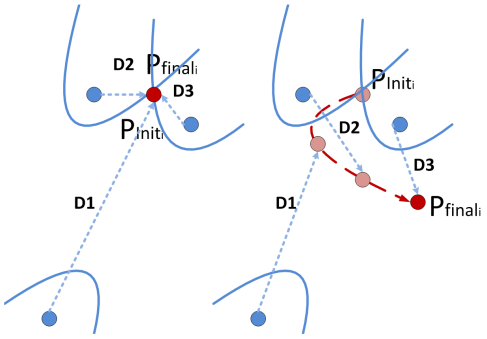

Fig. 1. Ranging error estimation between static node and mobile node

When the 3-WR procedure needs to be realized for each couple of nodes in the network, the traffic sent over the wireless medium increases rapidly with the number of nodes. In order to reduce this volume of traffic, the authors of [5] propose an algorithm called *Aggregated and Broadcast (A&B)* to limit the number of required handshake transactions. Each node that wants to acquire or refresh its position initiates the transaction by broadcasting a request packet to all its neighbors instead of querying a single node. After receiving multiple request packets, a node broadcasts a packet, which can contain multiple responses, and even a request. Compared to the classical peer-to-peer ranging (P2P) approach, A&B reduces the number of transmitted packets, and the delay between the acquisition of the four required distances. However, it can lead to a lower performance in presence of packet losses. An intermediate solution, peer-to-peer ranging with request broadcasting (P2P-B), which consists in broadcasting requests and transmitting responses one by one, constitutes a compromise between P2P and A&B.

This paper studies the impact of nodes mobility on the localization estimation and focuses on the MAC layer. We evaluate the impact of mobility on these various strategies using the WSNet discrete event simulator [6]. The nodes mobility pattern is defined by traces acquired through an experimental measurement campaign using a Vicon motion capture system. We also compare the effect on each algorithm's accuracy of the MAC-level scheduling of time slots

within a TDMA frame, which defines when requests and the corresponding responses are transmitted.

The remainder of the paper is organized as follows. In Section II, we present the system model and the mobility scenario. Section III describes localization strategies and the MAC scheduling we evaluate. Section IV presents and discusses simulation results.

II. System Model

A. Network Topology

We consider a single human body evolving in an indoor environment with a set of wireless devices attached to the chest, wrists, ankles and head of a body, as illustrated on Fig. 3(b). These nodes communicate through an IR-UWB physical layer. These devices operate with a single-channel frequency and are able to communicate with each other at one hop (mesh topology). We distinguish two categories of nodes. The first category regroups the *anchors nodes*, which are placed at the most static positions on the body (e.g. on the chest or on the back). Anchors define a *Local Coordinate System* (LCS). Note that the LCS is mobile and generally misaligned relatively to any Global Coordinate System (GCS). The second set of nodes comprises simple on-body nodes, whose positions are unknown and that need to be localized at least within the LCS. Localization is realized by estimating the distance between each anchors and the mobile node. In this paper, we denote by $\hat{d}_{ij}(t)$ the measured distance between node i and the anchor j at time t and by $\hat{P}_i(t)$ the estimated position of node i.

B. Ranging Estimation based on 3-WR

In this paper, the distance estimation is derived from the Time-Of-Arrival (TOA) measured for each involved packet and the 3-WR handshake protocol transactions. Figure 2 illustrates this classical exchange. The mobile node i, to be located, starts by sending a Request packet (Q_{ij}) to the anchor j at time T_1. After receiving this request at time T_2, the anchor j answers with a first Response packet ($R1_{ij}$) at time T_3. Node i receives this response packet at time T_4.

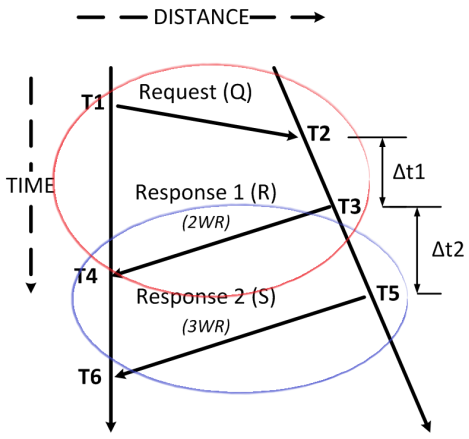

Fig. 2. Three Way Ranging Protocol

Note that, at this stage, the estimated ranging can be given through 2-WR as follows:

$\hat{d}_{ij}(t) = \frac{1}{2}c\,[(T_4 - T_1) - (T_3 - T_2)]$, where c is the speed of radio waves (i.e. $c = 3{*}10^8 m/s$). Given the time resolution of this process, the clock drift, which denotes the difference between the speed of a clock circuit and the absolute time, has impact on the time of flight estimation and consequently on the ranging accuracy. Indeed, clock drifts are not identical for each circuit and two nodes will not measure exactly the same time interval between two moments. To compensate this effect, the responding node j sends a second response packet at time T_5, which will be received by node i at time T_6. The resulting ranging estimate is computed as follows:

$$\hat{d}_{ij}(t) = \frac{1}{2}c\,[((T_4 - T_1) - \Delta t1) - ((T_6 - T_4) - \Delta t2)]\ , \quad (1)$$

where $\Delta t1$ and $\Delta t2$ are respectively equal to $(T_3 - T_2)$ and $(T_5 - T_3)$.

C. Mobility Model

To evaluate the effect of mobility on localization accuracy, we confronted the A&B and P2P-B algorithms to real mobility traces. These traces were obtained during a measurement campaign realized by the CORMORAN project carried out in June 2014 at the M2S laboratory of ENS Cachan, Bretagne, France.

The Vicon motion capture system [7], shown in action on Fig. 3(a), utilizes 16 high frequency (100 Hz) cameras surrounding a $10\,m \times 6\,m$ scene to record the position of multiple visual markers. We placed 41 markers on a human subject and 25 markers directly on the communication sensors carried by the subject, which allows us to acquire a very fine-grained history of the subject movements.

In this paper, we selected two particular scenarios to evaluate the impact of mobility on localization. In the first scenario, called *Yoga activity*, the subject realizes a series of static positions in the same place, mimicking Yoga postures (e.g. put both feet together and hands at the sides of the body, elongate the spine and fold forward from hips with knees, etc.). In the second mobility scenario, called *pedestrian walking*, the subject starts moving from the middle of the scene. Then, he walks at moderate speed along a rectangular trajectory centered on the starting point. Each capture lasts 100 s. More information on this campaign is available in [8].

III. Proposed MAC Strategies

Localization of the nodes placed on a body can easily suffer from the nodes mobility. Indeed, as nodes move constantly, their position evolves while estimating all required distances.

In this work, we only focus on the impact of nodes mobility on the localization accuracy. We therefore assume that the channel is perfect and we ignore the effect of shadowing and body obstruction. We consider, in the rest of the paper, a network composed of 8 devices, as represented on Fig. 3(b). Four fixed devices are positioned on the right of the chest (A1), the left of the chest (A2), the left hip (A3) and on the back

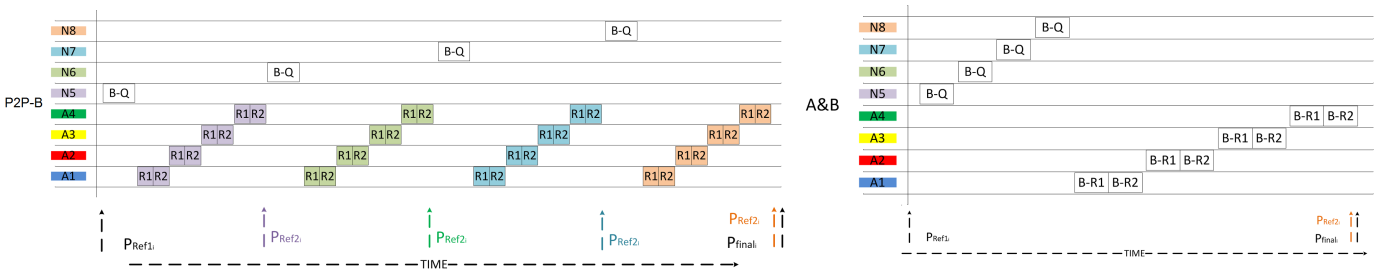

Fig. 4. Details of the P2P-B and A&B handshakes

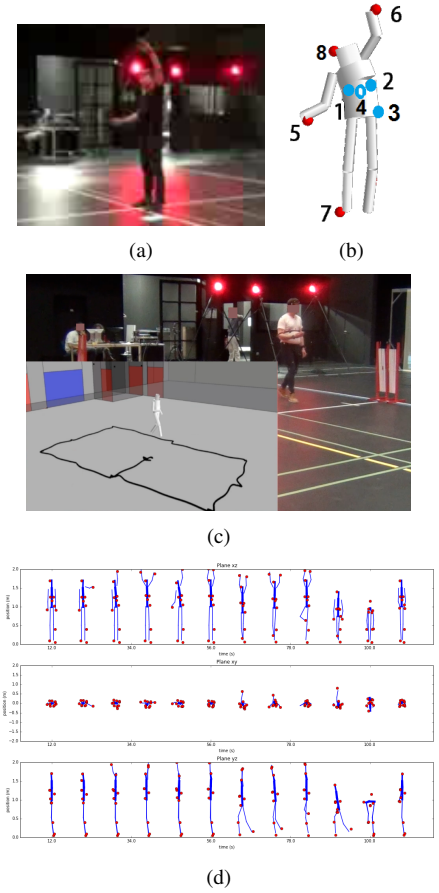

Fig. 3. (a) Subject camera recording for scenario of Yoga (b) Multi-cylinder Body reconstruction - the red (resp. blue) points refer to the mobile nodes (resp. anchors). (c) Pedestrian walking along a rectangular trajectory. (d) Decomposition of Mobility Model with PyLayers

(A4) and will play the role of anchors. Four mobile nodes are further positioned on the right arm (N_5), the left arm (N_6), the right foot (N_7) and the head (N_8).

A. Scheduling strategies based on 3-WR handshakes

To capture the body's movement accurately, the nodes positions should be refreshed at a frequency that corresponds to the movement speed. However, a basic and sequential implementation of the three-way ranging would require a request followed by two responses per link. The resulting control traffic can increase rapidly. Besides, when evaluated consecutively, the obtained distances will not refer to the same position, leading to positioning uncertainty. It is possible to reduce these impacts by grouping requests and responses in the same packet. Two such strategies are illustrated on Fig. 4:

- **Nodes are localized individually (P2P-B)**: a node i broadcasts a single request packet Q_i to all anchors. Each anchor then sends both responses ($R1_{ji}$) and ($R2_{ji}$) consecutively, one anchor at a time. Broadcasting the requests has the effect to increase, the $\Delta t1$ delay for some anchors. Besides, this delay is not uniform across the anchors.
- **Aggregated and Broadcast (A&B)**: in a first phase, all requests packets Q_i are transmitted in broadcast. Then, each anchor j sends an aggregated response ($R1_j$) to all nodes, followed by the second response ($R2_j$). A&B allows reducing the volume of traffic and hence the size of the TDMA frame, but also results in an increase of the $\Delta t1$ delay. However, in noisy environment with high packet-loss, its performance can be deteriorated.

One may note that the P2P-B favors the $\Delta t1$ delay (individual distance estimation), while A&B permits to obtain the four distances as fast as possible.

For these two strategies, we can derive the TDMA frame duration at the MAC layer. As depicted by Figure 5, P2P-B presents higher frame duration compared to A&B, which increases linearly with the number of nodes. This difference is explained by the number of packets sent by each protocol between m anchors and n mobile nodes. In A&B (resp. P2P-B), the nodes send n Request packets in Broadcast to the anchors. Then, the anchor nodes answer with m (resp. $n.m$) Response 1 packets and m (resp. $n.m$) Response 2 packets. Thus, we have $\Pi_{A\&B} = n + 2.m$ and $\Pi_{P2P-B} = n.(2m + 1)$ packets for A&B and P2P-B, respectively. Thus, in our scenario of 4 anchors and 4 mobile nodes, P2P-B presents a TDMA frame length of $\approx 54\,ms$ against $\approx 18\,ms$ for A&B. This means that for the duration of one P2P-B movement acquisition round, A&B can perform three times more the motion capture, and hence should reduce the impact of nodes mobility.

B. MAC-level slots scheduling

The strategies A&B and P2P-B both reduce the overall positioning time and save bandwidth, but delay the reception of the responses. It is however possible to play with the MAC-level scheduling (i.e. which slot of the TDMA frame is allocated to which emitter) to reduce the positioning error. The

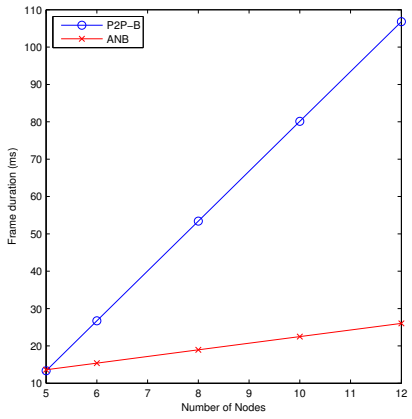

Fig. 5. Comparison of frame duration between P2P-B and A&B

MAC layer should therefore strive to reduce the $\Delta t1$ and $\Delta t2$ delays as much as possible, as shown in [9]. For the present scenario, involving 4 anchor nodes (A_1 to A_4) and 4 mobile nodes (N_5 to N_8), we evaluate and compare four MAC-level scheduling strategies, i.e. four different permutations of the slots allocated to each mobile node in the TDMA frame:

- **NS1** (N_5, N_6, N_7, N_8), where nodes with highest (resp. lowest) mobility are positioned at the beginning (resp. end) of the TDMA frame,
- **NS2** (N_8, N_5, N_6, N_7), where nodes with highest mobility are positioned in the middle of the TDMA frame,
- **NS3** (N_7, N_8, N_5, N_6), where nodes with highest (resp. lowest) mobility are at the end (resp. beginning) of the TDMA frame and
- **NS4** (N_6, N_7, N_8, N_5), where nodes with lowest mobility are positioned in the middle of the TDMA frame.

IV. Simulation and Results

A. Simulation environment

We compare the different algorithms and MAC-level scheduling strategies using the WSNet discrete-event simulator [6], which we modified to include simulation models that correspond to our scenarios. We implemented in WSNet a physical layer based on IEEE802.15.6 UWB [10] in default mode (OOK modulation and 0.4875 Mb/s). At the MAC, layer we implemented a TDMA-based medium access protocol, as well as the different algorithms and scheduling approaches, detailed in Section III. Finally, we implemented a mobility model that let us exploit the mobility traces acquired during the CORMORAN project, as detailed in section II-C.

Let us consider a mobile node i that performs κ localization operations throughout the simulation. At every localization attempt happening at date t, i computes an estimate position, $\hat{P}_i(t)$ that can be compared to the reference position, which can be the position occupied by the node the beginning of the 3-WR exchange ($P_{Ref_1}(t)$), at its end (($P_{Ref_2}(t)$)), or at the end of the TDMA frame ($P_{final}(t)$), as illustrated on Fig. 4. The accuracy of the localization process with respect to a given reference position is given by the root mean squared error (RMSE) of its estimate over the κ ranging operations realized throughout the simulation, expressed as follows for the reference position $Ref_r \in \{ref_1, ref_2, final\}$:

$$RMSE(i, ref_r) = \sqrt{\frac{\sum_{\kappa} \left(P_{Ref_r}(t) - \hat{P}_i(t) \right)^2}{\kappa}} \quad (2)$$

B. Impact of MAC-level scheduling on P2P-B accuracy

Let us first evaluate the impact of MAC-level slots scheduling of the different nodes on the localization accuracy. For this study, we evaluate the different parameters under a controlled scenario (e.g. Yoga) that we gradually accelerate by multiplying the speed of each on-body node multiplied by a factor 1 to 10 (1 corresponds to the real scenario).

Figure 6 shows the variation of the RMSE of the positions estimation according to the speed factor for each node MAC-level scheduling strategy presented in Section III-B with respect to the three references positions (P_{Ref_1}, P_{Ref_2} and P_{final}). As expected, the RMSE increases quasi-linearly with the speed factor. The distance covered during 3WR transaction increases with the node mobility, inducing more errors in the distance estimation and hence in the localization accuracy.

Figure 6(a) shows that the NS1 scheduling strategy yields to the best position estimation based on P_{Ref_1}. As nodes with higher mobility are placed at the beginning of the TDMA frame, their position is estimated at a moment closer to the reference instant. More static nodes, positioned later, will have moved less, which mechanically leads to a better RMSE. Similarly, NS3 scheduling, in which mobile nodes are scheduled at the end of the TDMA frame better estimates positions reached by the nodes at the end of the TDMA frame (P_{final}), as shown on Fig. 6(b). Fig 6(c) represents the positioning RMSE compared to the second reference positions, which corresponds to the end of the 3-WR exchange for each node. The different MAC scheduling strategies do not show much difference. P_{Ref_2} is therefore less sensitive to the MAC-level scheduling and should be a good candidate when no information on the individual nodes mobility is assumed.

C. Comparison of the MAC scheduling impact between P2P-B and A&B

Let us then compare the reaction of P2P-B and A&B algorithms presented in Section III-A to the slot scheduling strategy. This study relies on the same Yoga scenario as before. Estimations realized by the P2P-B and A&B are compared with the same reference positions.

Figure 7 compares the distribution of RMSE for all the allocation strategies for P2P-B and A&B. In Figure 7(a), we observe a significant gap between the different slot scheduling schemes with P2P-B when evaluating P_{Ref_1} or P_{final}. However, we can note that P_{Ref_2} remains the best estimated position, independently of the MAC scheduling. In the case of A&B, Figure 7(b) shows that the RMSE also presents a quasi-linear increase with the movement speed. Moreover, if

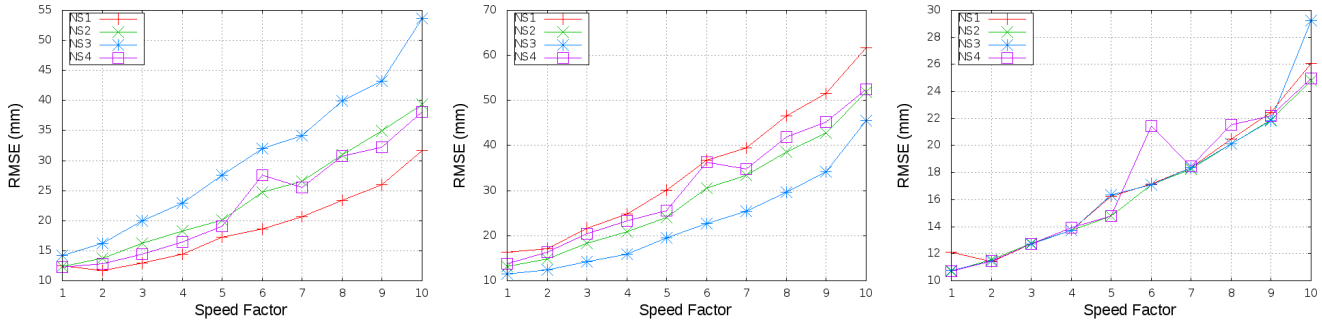

(a) RMSE respect to position P_{Ref_1} (b) RMSE respect to position P_{final} (c) RMSE respect to position P_{Ref_2}

Fig. 6. Impact of MAC-level scheduling on the P2P-B strategy

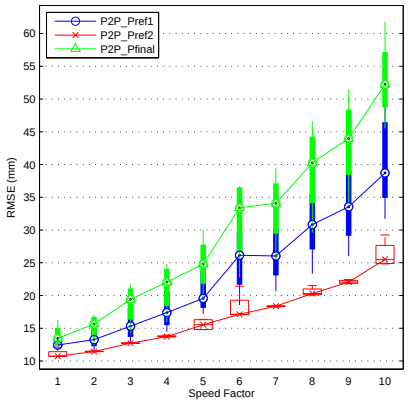

(a)

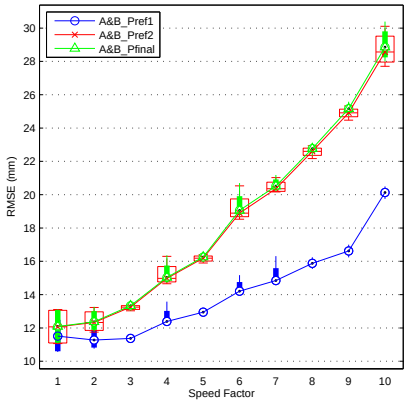

(b)

Fig. 7. Comparison of slots allocation strategies with (a) P2P-B and (b) A&B according to the estimation of the different reference positions

we compare the results between P2P-B and A&B (Fig. 7(b)), we observe that the impact of the MAC scheduling is limited for all reference positions. P_{Ref_1} becomes the best estimated position because $\Delta t1$ is considerably reduced. Therefore, A&B therefore tolerates more freedom with respect to the MAC scheduling.

On the basis of these results we identify the two extreme scenarios concerning the combination of the selection of the reference position and of the MAC scheduling strategy: i) the best case, where A&B (resp. P2P-B) performs the localization estimation according to P_{Ref_1} (resp. P_{Ref_2}) independently on the node slot strategy and ii) the worst case, where A&B and P2P-B perform the localization estimation with respect to P_{final} with mobile nodes scheduled at the very beginning of the TDMA frame NS1.

Finally, one can note that except for P_{Ref_2}, A&B permits to reduce the average error by a factor 2. Thus, the consistency in the 4 used distances is more important than the accuracy of each individual distances.

D. Quantification of position-related errors using P2P-B and A&B under different scenarios

In the two previous sections, we examined how the average positioning error evolved in function of the MAC-level scheduling and of the aggregation algorithm. Let us now look more closely at the distribution of the positioning error under the Yoga scenario as well as under the walking scenario detailed in section II-C.

Figure 8 presents the cumulative distribution function (CDF) of the on-body nodes position estimation error under both mobility scenarios. As expected, the positioning error distribution is dependent on the mobility scenario and on the handshake transaction protocol. The Yoga scenario (characterized by a low mobility) naturally presents a lower positioning error than the pedestrian walk scenario (characterized with a higher mobility). The level of improvement obtained by using the A&B protocol in place of the P2P-B protocol depends on the considered mobility scenarios: the gap between P2P-B and A&B in the case of walk scenario is bigger than the Yoga scenario. The performance of the "raw" P2P algorithm, which does not aggregate requests in a single broadcasted packet, is very close to the performance of P2P-B, which shows that a higher gain results from grouping answers rather than requests.

In the Yoga scenario, we observe that the difference between P2P-B and A&B is small. For the worst case (Fig. 8(a)), 90 % of positioning errors are smaller than 10 mm (resp. 20 mm) for A&B (resp. P2P-B) with an intersection point at $\approx 4\,mm$ for 70 % of errors. In the best case (Fig. 8(b)), 90 % of positioning errors are smaller than 5 mm (resp. 6 mm) for A&B (resp. P2P-B) with an intersection point at $\approx 4\,mm$ for 80 % of errors.

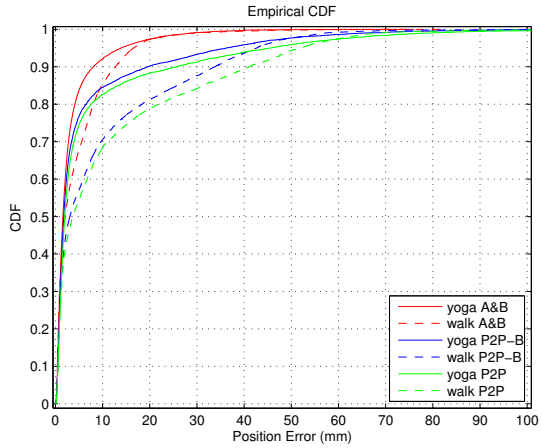

(a)

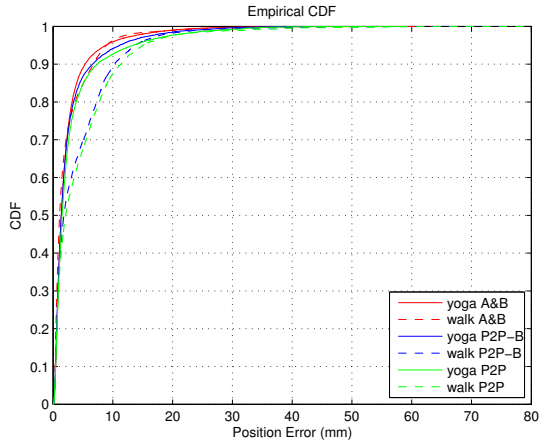

(b)

Fig. 8. Cumulative Distribution Function of the position error between P2P-B and A&B, considering a topology of 4 anchors and 4 nodes under the walking and yoga scenarios for the worst (a) and best (b) reference strategies

In the walking scenario, we notice a bigger gap between P2P-B and A&B. We observe that for the worst case (Fig. 8(a)) 90 % of error estimations are smaller than 15 mm (resp. 35 mm) for A&B (resp. P2P-B) with an intersection point at $\approx 3\,mm$ for 40 % of estimated errors. In the best case (Fig. 8(b)), 90 % of positioning errors are smaller than 8 mm (resp. 10 mm) for A&B (resp. P2P-B) with an intersection point at $\approx 1mm$ for 40 % of errors.

Table I reports the average positioning error in all situations. We can observe than A&B presents a gain of $\approx 50\%$ on the position estimation for the worst case under both mobility scenarios and a gain of 63% (resp. $90\,\%$) for the best case under the walking (resp. Yoga) scenario.

V. Conclusion

In this work we have quantified the impact of mobility on the positioning estimation with based on real and precise mobility traces. We have compared different strategies of slots allocation and we have shown that when anchors answer to the nodes individually (P2P-B strategy), it is more efficient to allocate the slots in the middle of the TDMA frame to estimate the instantaneous position. Moreover, A&B yields to a better performance than P2P-B in terms of latency and accuracy, with a better estimation of the position held by the sensor when the positioning request is sent. On the other hand, we have demonstrated that the Aggregated and Broadcast (A&B) mechanism reduces the impact of the slots allocation, which allows greater flexibility in the deployment of sensors on the body, and in potentially observable movements. These results are planned to be confirmed over a realistic propagation channel. We are also extending this study to other dynamic scenarios (e.g. running) and to the context multi-BAN for group navigation.

Mean Error (mm)	Worst Case		Best Case	
	P2P-B	A&B	P2P-B	A&B
Yoga	6.6	3.4	2.8	2.5
Walk	10.2	4.8	4.1	2.6

TABLE I
AVERAGE POSITION ESTIMATION ERROR IN THE WORST AND BEST CASES

Acknowledgment

This work has been carried out in the frame of the *COR-MORAN* project, which is funded by the French National Research Agency (ANR) under the contract number ANR-11-INFR-010. A part of this research has been realized at the LINCS laboratory. We thank all the involved researchers from ENS/IRISA and M2S Lab for their precious support during the measurement campaign.

References

[1] S. Ullah, M. Mohaisen, and M. A. Alnuem, "A review of IEEE 802.15.6 MAC, PHY, and security specifications," *International Journal of Distributed Sensor Networks*, pp. 1–12, 2013.

[2] M. Hamalainen, A. Taparugssanagorn, and J. Iinatti, "On the WBAN radio channel modelling for medical applications," in *Antennas and Propagation (EUCAP), Proceedings of the 5th European Conference on*, pp. 2967–2971, 2011.

[3] Z. Xiao, Y. Hei, Q. Yu, and K. Yi, "A survey on impulse-radio UWB localization," *Sci. China Inf. Sci.*, vol. 53, pp. 1322–1335, Jul 2010.

[4] J. Hamie, B. Denis, R. D'Errico, and C. Richard, "On-body toa-based ranging error model for motion capture applications within wearable UWB networks," *Journal of Ambient Intelligence and Humanized Computing*, Dec 2013.

[5] D. Macagnano, G. Destino, F. Esposito, and G. Abreu, "MAC performances for localization and tracking in wireless sensor networks," *2007 4th Workshop on Positioning, Navigation and Communication*.

[6] G. Chelius, A. Fraboulet, and E. Ben Hamida, "http://wsnet.gforge.inria.fr/."

[7] "Vicon." http://www.vicon.com/.

[8] B. Denis, N. Amiot, B. Uguen, A. Guizar, C. Goursaud, A. Ouni, and C. Chaudet, " Qualitative Analysis of RSSI Behavior in Cooperative Wireless Body Area Networks for Mobility Detection and Navigation Applications," in *21st IEEE International Conference on Electronics Circuits and Systems*, (Marseille, France), Dec. 2014.

[9] A. Guizar, A. Ouni, C. Goursaud, N. Amiot, and J. Gorce, "Impact of MAC scheduling on positioning accuracy for motion capture with UWB body area networks," *Proceedings of the 9th International Conference on Body Area Networks*, 2014.

[10] "IEEE standard for local and metropolitan area networks - part 15.6: Wireless body area networks," 2012. IEEE Std 802.15.6-2012.